Fully Kinetic Particle-in-Cell Simulation of a Hall Thruster

Francesco Taccogna[1], Savino Longo[1,2], Mario Capitelli[1,2], and Ralf Schneider[3]

[1]Dipartimento di Chimica dell'Universitài di Bari, via Orabona 4, 70126 Bari, Italy
cscpft61@area.ba.cnr.it
[2]IMIP-CNR, sect. Bari, via Orabona 4, 70126 Bari, Italy
[3]Max Planck Institute für Plasmaphysik, Wendelsteinstr. 1, D-17491 Greifswald, Germany

Abstract. A 2D axisymmetric fully kinetic Particle-in-Cell (PIC) model of the atom (Xe), ion (Xe^+) and electron dynamics of a stationary plasma thruster (SPT) is developed. Electron-neutral elastic scattering, excitation and ionization processes are modelled by Monte Carlo collision methodology. The interaction of the plasma discharge with the ceramic walls leads to plasma recombination, energy loss and secondary electron. These phenomena are included into the model by different approaches. The electric field is self-consistently solved from the Poisson equation, while the magnetostatic field is precomputed. The code is applied to a scaled SPT thruster geometry where fundamental physics parameters are kept constant. The model reproduces the discharge ignition dynamics. The numerical results will provide a better understanding of the experimentally observed enhanced axial electron current and high frequency oscillations.

1 Introduction

The modelling of electric thruster is a very important issue in view of the increasing importance of such propulsion in all space applications when specific impulse, and not just power, is important, i.e. for satellite guidance, orbit transfer and deep space exploration projects.

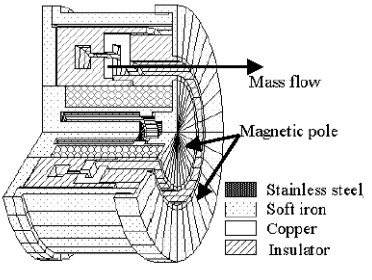

Fig. 1. Schematic representation of the discharge chamber in the SPT-100 thruster

M. Bubak et al. (Eds.): ICCS 2004, LNCS 3039, pp. 588–595, 2004.

A SPT can be schematically described (see Fig. 1) as an anode-cathode system, with a dielectric annular chamber where the propellant ionization and acceleration process occurs [1]. This thruster works using a perpendicular electric and magnetic fields configuration. A magnetic circuit generates an axisymmetric and quasi-radial magnetic field between the inner and outer poles. In operation, an electrical discharge is established between an anode (deep inside the channel), which is acting also as a gas distributor, and an external cathode, which is used also as an electron emitter. In this configuration, cathode electrons are drawn to the positively charged anode, but the radial magnetic field creates a strong impedance, trapping the electrons in cyclotron motion which follows a closed drift path inside the annular chamber. The trapped electrons act as a volumetric zone of ionization for neutral propellant atoms and as a virtual cathode to accelerate the ions which are not significantly affected by the magnetic field due to their larger Larmor radii. Generally, xenon is used as propellant. The quasi-radial magnetic field and the channel length L are chosen so that:

$$\begin{aligned} r_{L,e} &<< L << r_{L,i} \\ \omega_{c,i}\tau_i &<< 1 << \omega_{c,e}\tau_e \end{aligned} \tag{1}$$

where r_L is the Larmor radius, ω_c is the angular cyclotron frequency, τ is the mean time between collisions and the subscripts e and i means electrons and ions. Electrons are strongly magnetized, whereas ions are non-magnetized. The resulting external jet composed by the high speed ion beam is subsequently neutralized by part of electrons coming from the external cathode-compensator. The presence of an insulator as wall material has a profound effect on the plasma within a Hall type thruster. After an impact with dielectric walls, high energy electrons are absorbed and release less energetic secondary electrons that are more firmly confined by the magnetic field. The result is that the dielectric wall limits the temperature of the electrons confined into the channel. By limiting the electron temperature, a smooth continuous variation of the plasma potential results. These effects will be specially addressed within this work.

Models of Hall thrusters have been developed using hybrid fluid-particle approaches [2-7] to aid in the optimization of the performance of the thruster. In all these models, electrons are described as a fluid by the first three moments of the Boltzmann equation. They are 1D (axial or radial), quasi-1D (considering wall losses) or 2D (in the plane (r,z) or (r,θ)), and steady-state or transient (on the ion time scale). Most of the models are based on the quasi-neutrality (QN) assumption. Therefore, Poisson's equation is not solved and the constraints related to the explicit time integration of the transport equations and explicit space integration of the Poisson's equation were therefore eliminated. This assumption considerably simplified the numerical aspect of the simulation. Usually, in the electron momentum transport equation, Bohm and/or near-wall conductivity were included by means of empirical fitting parameters. A question which cannot be resolved by these models, and which in fact strongly limits the reliability of their results, is the electron transport in SPTs, and in particular the important role that the electron interactions with the channel walls play together with volume processes. As a result,

SPT performance is affected by both the state of the wall surface and the properties of plasma structures on Debye and electron-Larmor scales. Therefore, the construction of a self-consistent theory of SPT processes requires a kinetic description of not only heavy particles (atoms and ions), but of electrons as well. To accomplish this, we present a two-dimensional axisymmetric Particle-In-Cell (PIC) [8,9] model using Monte Carlo Collision (MCC) method to take into account electron-neutral interactions. Secondary electron emission from the wall is simulated by a probabilistic model [10]. The electric potential is calculated solving Poisson equation solution without assuming quasi-neutrality.

We first describe in Sec. 2 the numerical model. The results are presented and discussed in Sec. 3.

2 Numerical Method

2.1 Geometrical Scaling

To capture electron dynamics, we need a time-step on the order of the plasma oscillation. Unfortunately, using the real mass ratio, neutral particles will require millions of such time-steps to cross the simulation region. In order to speed-up the code we have reduced the dimension of the discharge while preserving the values of the relevant parameters that govern the physics [11]. All the basic plasma characteristics in gas-phase ionization devices rely heavily on the ionization process, whereby the neutrals are ionized in collisions with the electrons. As the size of the device is reduced, everything else remaining constant, the number of collisions that the electrons and the neutrals experience with each other as they traverse the effective length of the device is reduced. Thus, in order to maintain the effective collision probability, it is necessary to increase the number densities of all the species in proportion, that is the mass flow rate of propellant should scale as:

$$\dot{m} = M_{Xe} n_N c_s A \sim L \tag{2}$$

where M_{Xe}, n_N and c_s are the neutral mass, density and thermal velocity respectively, while A is the area of the anode. Moreover, to preserve the effectiveness of the electron confinement scheme (the ratio of the Larmor radius to the thruster dimension) under scaling, the strength of the magnetic field must vary inversely with length. The discharge current I_d, determined as the product of the current density times the area of the device, scales proportionally with length. Consequently the thrust T, that is the total force undergone by the SPT in reaction to the acceleration of the ions, scales linearly with the length while the specific impulse $I_{sp} = T/\dot{m}g$ remains invariant under geometrical scaling. Here we have assumed that the electron temperature is constant and independent of scale, as was shown in Ref. [11]. However, the benefits of this trick are limited. First, the plasma frequency must remain shorter than the electron gyrofrequency. Also, the Debye length must remain a small quantity with respect to overall thruster dimensions. If the sheaths become too large, they can interfere with the discharge. Under these constraints the geometrical reducing factor was ζ=0.02.

2.2 Magnetic Field

Because the self-induced magnetic field is negligible compared to the applied field from the Hall thruster's coils, the simulation uses only a constant magnetic field. Under this condition we can define the magnetic potential ϕ_B and use the corresponding Laplace equation to solve for the magnetic field. Boundary conditions are the same used by Fife [3]: at the right and left boundaries, one has zero flux, while on the outer magnetic pole, one has $\phi_B = 1$, and on the inner pole one has $\phi_B = 0$. We then solved for ϕ_B across the domain, and took the gradient to arrive at the magnetic field **B**. Finally, we specified a control point and a field strength at that control point, and used that to normalize the field.

2.3 Neutral Gas Particle Kinetics

The neutral density in this test case is two order of magnitude higher than the plasma density. Therefore we let neutral super-particles be some integral number s_N=100 times larger than plasma super-particles. As a neutral undergoes ionization events, s_N decreases by one unit until s_N=0 and the particle disappears. We initialize the simulation by expanding a plume of neutrals from the anode with a long time-step until we approach a steady state. The number of neutrals macroparticles created at the anode line (z=0) per time-step Δt_N, is a function of the scaled mass flow rate according to:

$$\Delta N_N = \frac{\dot{m}'}{M w_N} \Delta t_N \tag{3}$$

where w_N is the neutral statistical weight. They are injected with a radial position sampled from an uniform cylindrical density distribution and their initial velocity distribution is taken to be half-Maxwellian with a temperature of typically 500 K, by using the polar form of the Box-Muller transformation for velocity. Neutrals can disappear when they reach the right boundary of the geometry. Neutrals which hit the anode and walls are re-emitted according to an half-Maxwellian at a wall temperature (900 K) based on experimental data. One must consider the probability for a particle crossing the surface to have a given direction. This probability density actually follows a cosine law, due to the fact that particles with a large velocity component along the normal to the surface escape more frequently than others. The probability densities for axial and azimuthal velocity components are Gaussian distribution (the polar form of the Box-Muller transformation was used), while the probability density for the radial component is a Rayleigh distribution. Neutral-neutral collisions may be ignored, assuming a neutral free molecular regime because the mean free path is much longer than thruster dimension.

2.4 Plasma Phase

When neutral particles have filled the simulation region, electrons are introduced each time step Δt from the exit plane (the cathode is not included in the simulation region) with a steady state current control method of electron injection [12]:

$$n_e = \frac{I_d \, t}{qw} - n_i^c + n_e^c \tag{4}$$

where w is the statistical weight of electron super-particles, q is the elementary charge, Δn_i^c and Δn_e^c are the number of ions and electrons passing the free space boundary each iteration. Electron initial velocity distribution is taken to be half-Maxwellian with a temperature of typically about 15 eV. They can lose energy and change momentum by collisions (elastic scattering, excitation and ionization) with neutrals. These interactions are modelled by MCC technique and scattering cross sections are gathered from the literature [12]. For each electron we calculate the probability of an e-N scattering in a time Δt_{coll} short with respect to the mean free flight time:

$$P_{tot} = n_N \sigma_{tot}(v_e) v_e \Delta t_e = \sum_{k=1}^{3} n_N \sigma_k(v_e) v_e \Delta t_e = \sum_{k=1}^{3} P_k \tag{5}$$

where n_N is the neutral density, σ_{tot} is the total electron-neutral cross section, v_e is the electron velocity and P_1, P_2 and P_3 are the probability for the occurrence of collisional event 1, 2, and 3, respectively. P_{tot} is compared with a random number r_d sampled from an uniform distribution in the range [0,1] in order to decide if a collision event happens (in our case Δt_{coll} is chosen so that $P_{tot}<10^{-2}$). If $P_{tot}>r_d$, we compare another random number to the cross sections for elastic scattering, excitation, and ionization to determine which type of event occurs. We choose the collisional event j if

$$\sum_{k=1}^{j-1} \frac{P_k}{P_{tot}} < r_d \leq \sum_{k=1}^{j} \frac{P_k}{P_{tot}} \tag{6}$$

In all cases, the electron is scattered isotropically. If the collision is inelastic, energy (8.32 eV for the first excitation and 12.1 eV for the first ionization) is subtracted from the electrons. In the case of ionization, ions and secondary electrons are created at the primary electron's location. The energy of primary and secondary electrons is divided randomly.

When an electron strikes the dielectric wall (Boron Nitride BN), we decide the number of electrons emitted on the basis of the energy and the angle of impact of the incident electron implementing the probabilistic model of Furman and Pivi [10]. The energy spectrum of the emitted electrons is able to reproduce the three different type of secondary electrons, that is backscattered (high energy region), rediffused (middle energy region) and true secondary electrons (low energy region). For simplicity, we assume the same emission-angle distribution (~cosθ and uniform azimuthal angle) for all electrons, regardless of the physical mechanism by which they were generated.

Verboncoeur interpolation method [13] which guarantees charge density conservation on a radial metrics is used to weight particles to the grid nodes, where

the field equations are solved, and to weight the fields back to the particles. The electric potential is re-calculated each time-step using finite differences method for Poisson equation which is solved iteratively using successive over-relaxation (SOR) with Chebyscev acceleration technique [8]. As regards the boundary conditions, we keep the electric potential constant at the anode and at the exit plane and we also assume that the electric field changes its sign at the dielectric surface and its magnitude remains the same [14]. Then, the boundary condition at the walls can be written as:

$$E_w = -\frac{\rho}{2\varepsilon_0} \tag{7}$$

where ρ is the surface charge density and ε_0 is the free space permittivity constant; the possible surface conductivity of the dielectric is neglected. The potential at the wall surfaces is assumed to be zero. Electrons are moved discretizing the equations of motion by the leapfrog method of Boris [9]. All electrons which hit the anode boundary and the free space boundary are deleted. At the end of each electron loop, ions are created at the ionization locations. The initial ion velocity is set equal to the local neutral background velocity, but ions and neutrals are moved once each 100 electron loop. An ion which impacts the anode and the walls disappears and a neutral is created with one half of the ions initial kinetic energy, but with a random velocity direction. The particle is thus partially accommodated in energy, and fully accommodated in momentum. At the free space boundaries, all particles are deleted and a count of electron, ion and neutral fluxes is maintained.

3 Results and Discussions

In this section, we present the simulation results (scaled values) at the following operating conditions: channel length L=2.5 cm, inner radius R_{in}=3.5 cm, outer radius R_{out}=5 cm, discharge voltage ϕ_d=300 V, mass flow rate $\dot{m} = 3\,\mathrm{mg/s}$, discharge pressure P=2x10^{-5} mbar, discharge current I_d=3.2 A, maximum radial magnetic field $B_{r,max}$=150 Gauss.

Figure 2(a) shows long time history of electron, ion and neutral total number macroparticles. We can see that charged particles continue to oscillate (the simulated discharge is not stable), while the number of neutrals is not strongly changed due to the fact that one neutral transit time corresponding to the simulation time is not sufficient to see the low frequency phenomena related to the neutral scales.

The colour plots of Figs. 2(b)-3 demonstrate the main features of the discharge and show, respectively, the space variation of the electric potential, plasma density and electron temperature. As it can see in Fig. 4(b), most of the potential drop occurs in the exhaust region, where the magnetic field is large. This decrease compensates the low electron conductivity in this region and ensures current continuity. It is customary to allocate the acceleration region here. The large axial electric field resulting from this voltage drop is responsible for accelerating the ions from the ionization region to the exit plane and the electron from the outlet to the

anode. From the figure, also the little anode drop (~20 V) and the lateral wall sheaths, whose voltage drop decreases from the anode to the outlet, are evident. However, the computed potential vanishes at the channel exit, while observations [15] indicate that only one-half to one-third of the potential drop takes place downstream of the thruster exit. This difference is due imposing the zero potential boundary condition at the exit plane in the numerical simulation, i.e., the full potential drop is forced to occur inside the channel.

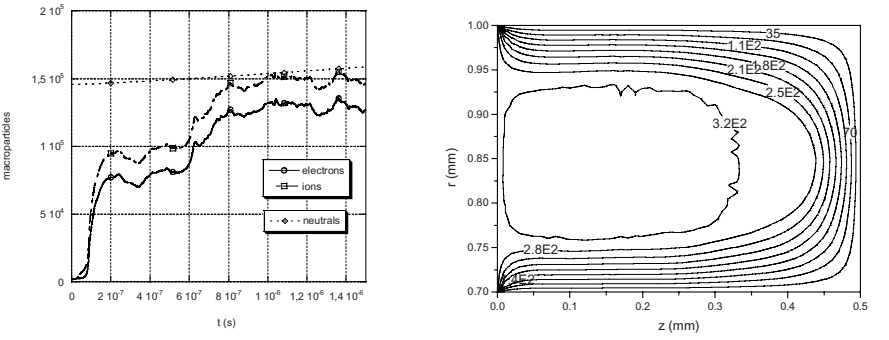

Fig. 2. (a) Long time history of electron, ion and neutral macroparticles. (b) Profile of the plasma potential

The space variation of the plasma density (Fig. 3.a) shows that the plasma reaches its maximum in the center of the channel and in the ionization region, while it decreases in the acceleration region due to the increasing ion velocity. The electron temperature (Fig. 3.b), calculated in each cell from the usual formula reaches a maximum (18 eV) close to the exhaust and decreases to about 6.7 eV in the low electric field region. The peak can be attributed to Ohmic heating due to the maximum azimuthal drift velocity in this region. Furthermore, the drop near the walls is a consequence of the emission of cold secondary electrons from the insulators. These numerical results are consistent with our global understanding of the stationary plasma thruster and reproduce quite well the experimental observations [15].

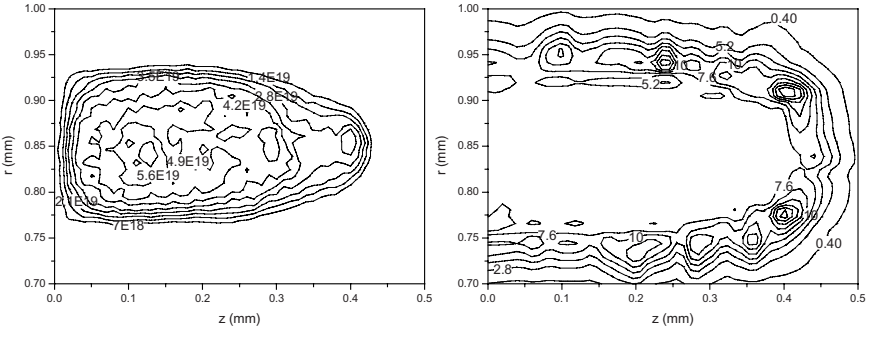

Fig. 3. Profile of the electron (a) density and temperature (b)

5 Conclusions

A 2D(r,z)-3V numerical model was developed to assess the effect of dielectric walls in stationary plasma thrusters. The model consists of a fully kinetic PIC-MCC for the plasma phase. The emission of secondary electron by electron impact from the walls is taken into account by a probabilistic model simulating the different kind of electrons created at the wall, backscattered, rediffused and true secondaries. In order to make the simulation possible and model the electron dynamics, a new kind of scaling-law is applied for the PIC model.

References

1. Zhurin, V. V., Kaufman, H. R., Robinson, R. S.: Plasma Sources Sci. Technol. 8 (1999) R1.
2. Komurasaki, K., Arakawa, Y.: J. Prop. Pow. 11(6) (1995) 1317.
3. Fife, J. M.: PhD thesis, Massachusetts Institute of Technologies (1998).
4. Hagelaar, G. J. M., Bareilles, J., Garrigues, L., Bœuf, J.-P.: J. Appl. Phys. 91(9) (2002) 5592.
5. Koo, J. W., Boyd, I. D.: AIAA paper 2003-10113 (2003).
6. Garrigues L. : PhD thesis, Université Paul Sabatier, Toulouse (1998).
7. Levchenko I., Keidar M.: IEPC-2003-162 (2003).
8. Eastwood, J. W., Hockney, R. W.: Computer Simulation using particles, McGraw-Hill, New York (1981).
9. Birdsall, C. K., Langdon, A. B.: Plasma Physics via Computer Simulation, Mc-Graw-Hill, New York (1985).
10. Furman, M. A., Pivi, M. T. F.: Phys. Rev. Special Topics – Accel. and Beams 5(12) (2002) 124404.
11. Khayms, V.: PhD thesis, Massachusetts Institute of Technology (2000).
12. Szabo, J. J. Jr.: PhD thesis, Massachusetts Institute of Technology (2002).
13. Verboncoeur, J. P. : J. Comp. Phys. 174 (2001) 421.
14. Morozov, A. I., Savel'ev, V. V.: Plasma Phys. Rep. 28(12) (2002) 1017.
15. Bishaev, A. M., and Kim, V. P.: Sov. Phys. Tech. Phis. 23 (1978) 1055.